A SURVEY OF INSTRUMENTS AND EXPERIMENTS FOR X-RAY ASTRONOMY

(Invited Discourse)

HERBERT GURSKY
American Science and Engineering, Cambridge, Mass., U.S.A.

1. Introduction

A diversity of instruments have been utilized or proposed for use in X-ray astronomy. This in part reflects the fact that the field is very new, that many competing techniques have been devised for any given type of observation and that there has been a progression to increasingly sophisticated instruments. But most of this diversity is real and simply reflects the very broad range of observations that can be performed and the different kinds of observational opportunities that are presented to the several experimental groups. Useful measurements are being performed over three decades of energy extending from 0.25 keV to 500 keV, positional measurements extend from degrees to arc seconds precision, attempts have been made to measure the polarization of the X-ray sources, time variations are being studied and spectra are being measured to resolutions of the order of $\sim 20\%$. The required instruments are being flown on sounding rockets, balloons and satellites. In addition, observation of the diffuse X-ray backgrounds requires even different instruments.

These essential elements of an X-ray astronomy experiment can be reduced to the following items, a collimating device (baffles, wires, focussing devices), a beam conditioner (filters, polarizer, grating) and a detector (proportional counter, photoelectric detector). These units must be mounted rigidly on the carrier (rocket, balloon). Some means must be provided to maneuver or point the carrier in order to acquire or sweep by the X-ray sources or other interesting regions of the sky. Since it is necessary to know where in the sky one is looking, some means of determining celestial attitude must be provided for. Finally, there is the problem of signal conditioning and the return of data to the ground. The essential elements of an X-ray astronomy experiment are shown in Figure 1.

The design of the instrumentation used in X-ray astronomy is very much dependent on some model of the X-ray sky; namely, the distribution and intensity of the sources in the sky, the spectral distribution of the radiation, the effect of the interstellar medium on the radiation and the nature and intensity of the non-X-ray background. Furthermore, the instrumental developments depend a great deal on certain notions we have regarding the nature of the sources; i.e., will the radiation be polarized, will spectral lines be present, are the sources of small or large angular size.

A number of review articles on X-ray astronomy have appeared within the past year; two which deal entirely with instrumentation are by Giacconi *et al.* [1] on

L. Gratton (ed.), Non-Solar X- and Gamma-Ray Astronomy, 5–33.

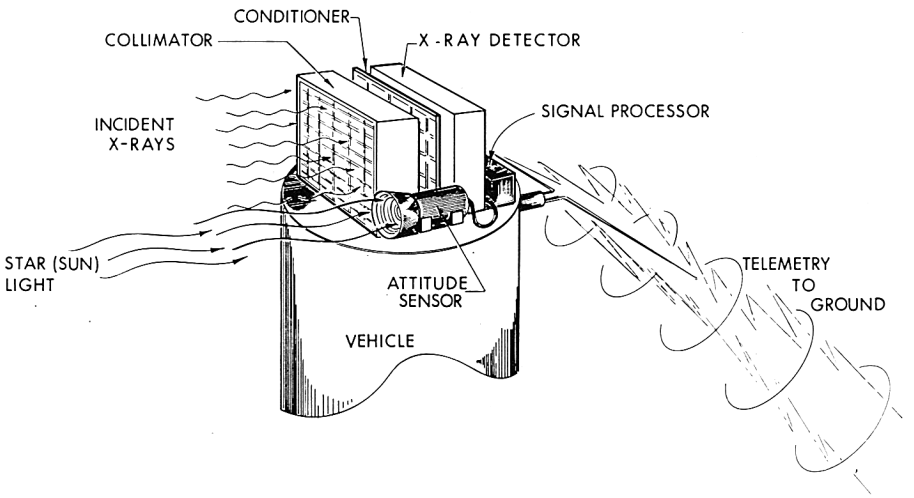

Fig. 1. Elements comprising the X-ray astronomy experiment. In addition to those shown there is normally some means of stabilizing the vehicle.

TABLE I

Anticipated distribution of X-ray sources

	Distance	Number	Intensity (Relative to the Crab Nebula)	Angular Size
Supernova remnants:				
Crab Nebula	1700 pc	1	1	3′
	10 kpc	40	3×10^{-3}	30″
	500 kpc (M31)	100	10^{-5}	0.5″
Sco X-1 like objects:				
Sco X-1	~ 1000 pc	1	10	small
	10 kpc	10^3	10^{-2}	
	500 kpc (M31)	2×10^3	4×10^{-5}	
Stellar corona:				
Sun	5×10^{-6} pc	1	10^7	
	10 pc	10	2×10^{-6}	small
Extragalactic sources:				
M-87	1.1×10^7 pc	1	5×10^{-2}	1′
	1.1×10^8	10^3	5×10^{-4}	6″
	1.1×10^9	10^6	5×10^{-6}	0.6″

conventional techniques and by Giacconi *et al.* [2] dealing exclusively with applications of X-ray telescopes.

2. A Model of the X-Ray Sky

The distribution of X-ray sources on the celestial sphere is shown in Figure 2. The striking feature of this distribution is the concentration of sources along the Milky

https://doi.org/10.1017/S0074180900003971 Published online by Cambridge University Press

Way with the highest concentration being within $\sim 20°$ longitude of the galactic center. The galactic sources comprise at least two types; in the first place, there are supernova remnants like the Crab Nebula and Cas A which are of large angular size, and secondly there are the star-like objects as exemplified by Sco X-1 and Cyg X-2. The latter are probably highly variable in intensity while the former are probably stable. The range of intensity of the observed galactic sources is between $10\times$ and $0.1\times$ that of the Crab Nebula (20–0.2 photons/cm^2-sec in the 2–10 keV energy range). The intrinsic luminosity of these sources is in the range 10^{36}–10^{37} ergs/sec. In addition, we have good evidence for the existence of a class of X-ray galaxies as exemplified by M-87. In Table I, I present what might be expected for a number – space density of these sources. Also, one must consider the sun as an X-ray source, even though the study of solar X-radiation is not normally considered within the province of X-ray astronomy. The reason is simply that at some level of sensitivity, stellar corona in nearby

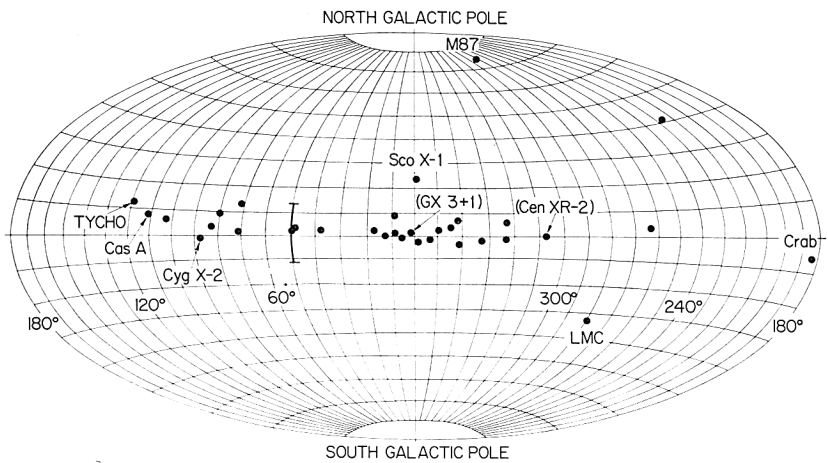

Fig. 2. Distribution of known X-ray sources in the galactic coordinate system.

TABLE II

Low energy cutoffs due to the interstellar medium

	E-cutoff[a]
Extragalactic objects:	
Pole	0.2 keV
60° latitude	0.3
30° latitude	0.44
Galactic objects:	
in the plane	
10 pc	0.12 keV
1 kpc	0.7
10 kpc (toward galactic center)	3 keV

[a] Energy at which the optical depth is unity.

https://doi.org/10.1017/S0074180900003971 Published online by Cambridge University Press

stars will be observable and that techniques used in solar studies are being adapted for use in X-ray astronomy.

The significance of the data in Table I is that with modest improvements in sensitivity (~factor 10–100) over what is now being achieved one may have a very great increase in the number of observable sources, and when and if sensitivity can be improved 4–5 orders of magnitude we can expect qualitatively new phenomena to reveal themselves, such as the observations of X-ray sources at cosmological distances, of 'common' X-ray sources in nearby galaxies, and of the coronal emission of nearby stars. One point that must be mentioned is that increased sensitivity requires the use of high resolution collimators in order to avoid the problem of source confusion. Even now, mechanical collimators are inadequate to clearly separate the sources at low galactic longitudes. With very high sensitivities it is apparent that instruments with arc second resolution are called for; e.g., the 1000 or so sources in M-31 would be distributed over less than 1 $(\text{deg})^2$.

The spectral composition of the radiation, as modified by the interstellar medium, has an important bearing on instrument design. In the first place, the spectral intensity characteristically falls off with increasing energy either as power laws or as exponentials. Thus, the largest number of photons are always present at the lowest energy. However, the interstellar medium limits how low in energy measurements can be performed, depending on the distance to the sources. Based on calculations of Bell and Kingston [3], the cutoff energies are shown in Table II. These values are uncertain to the extent that we do not yet know the X-ray absorbing characteristics of the interstellar medium. The results of Bowyer *et al.* [4], which apparently have been confirmed by Kraushaar's group at the University of Wisconsin, indicate that the X-ray absorbing characteristics at 0.28 keV and at high galactic latitudes are lower by about a factor of 3 compared to the calculations in Table II. But the qualitative features of the interstellar absorption are unchanged; namely, that at high galactic latitudes, significant fluxes of radiation can be recorded at 0.3 keV, while in the plane, the cutoffs will lie between 3 or 4 keV and 0.7 keV depending on the location of the source. It is also possible that absorbing material may be present in or near the X-ray sources themselves. Furthermore, if one is content to study the X-ray emission from the nearest 100 or so stellar objects, observations can be extended to at least 0.1 keV, which means that coronal emission can be observed.

3. X-Ray Detectors

A. 1–20 KEV X-RAY

Up to now, this energy range has provided the bulk of the information on the X-ray sources and the background. The principal detector is the gas proportional counter using a window of beryllium or organic films such as mylar. Calculated efficiencies for typical counters are shown in Figure 3. The beryllium window counters have the advantage in that they can be entirely gas tight which gives long shelf-life and the capability of extended life in orbit. The organic films are typically porous to certain

gases which limits their life unless special precautions are taken such as continuous renewal of the counter gas.

The state-of-the-art of gas proportional counters has advanced to the point that it is possible to construct counting systems which are virtually free from any counting

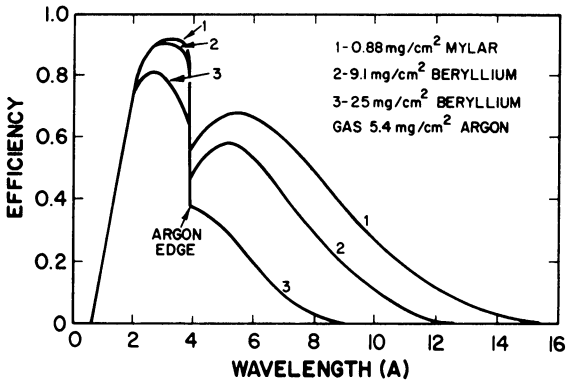

Fig. 3. The efficiency of gas proportional counters using argon as a filling gas. Efficiency can be extended to shorter wavelengths by the use of higher pressure of argon, or the use of heavy gases such as xenon and krypton.

background other than X-rays entering the front window, particularly through the use of pulse shape (or rise time) discrimination, which has allowed a significant improvement in sensitivity for experiments using proportional counters. This technique was first introduced into X-ray astronomy experiments by Dr. Pound's group at Leicester [5], and has been extended by Gorenstein and Mickiewicz [6]. It permits the rejection of counter signals originating from minimum ionizing electrons such as arise from cosmic rays traversing the counter or γ-rays converting in the walls. These events, the latter especially, form the principal non-X-ray background in most experiments.

The basis for pulse shape discrimination is that counter signals arising from X-rays form a narrow spread in pulse rise time; whereas signals coming from γ-rays have a very large spread in rise times, up to 10 times those of X-rays. Thus if one electronically selects events (of a given amplitude) on the basis of their rise time a large fraction of the non-X-ray events can be rejected – up to 99% in certain instances. Figure 4 shows actual performance in a flight experiment of PSD. In this case we estimated that the residual, non-X-ray background was reduced to $\sim 10^{-2}$ cts/cm^2-sec for the projected area of the detector. In principle, one should be able to reduce non-X-ray counts even further by the incorporation of several background rejection techniques; e.g., PSD, guard counters and wall-less detectors (the latter are detectors in which the anode is replaced by a grid and the guard counter is incorporated into the primary counter). In practice, however, the limit on the background counting rate is frequently determined by the diffuse X-ray background which of course can not be discriminated against within the detector.

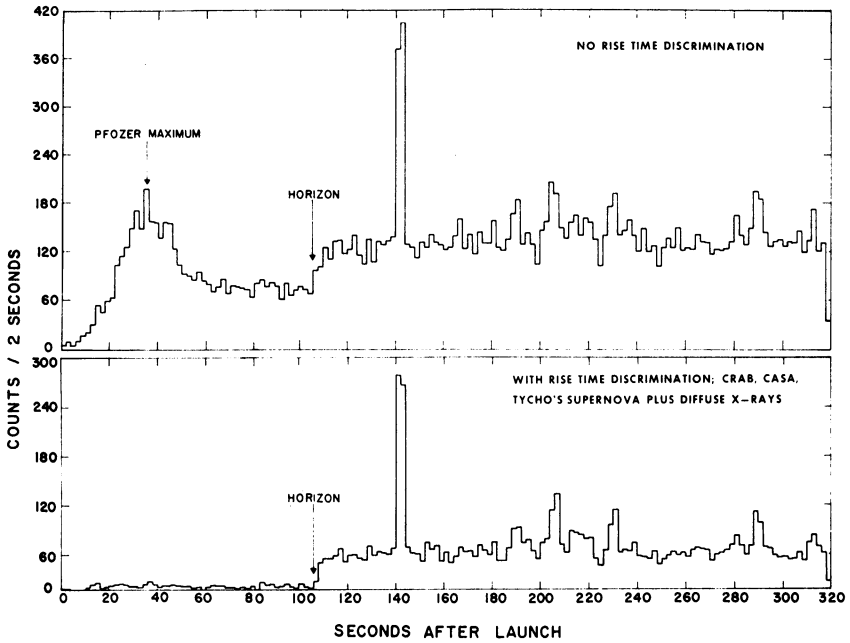

Fig. 4. The effective pulse shape discrimination during an AS & E sounding rocket flight using a system developed by Gorenstein and Mickiewicz. The residual counting rate at times greater than 100 sec is almost entirely the result of the diffuse X-ray background plus individual point sources of X-rays.

B. HARD X-RAY DETECTION

The response of proportional counters can be extended to ~ 50 keV by using heavy filling gases such as xenon and krypton operating at high pressures. To detect higher energies it is necessary to use scintillation counters with NaI(Tl) being the most common choice of a scintillating crystal. Observations have been made to several hundred keV with NaI scintillation counters on discrete sources and to several MeV on the diffuse background.

The extraneous counting rates represent a very severe problem at these higher photon energies. The cosmic photon fluxes fall off with increasing energies much faster than the extraneous radiation.

The latter is most likely to be photons produced by compton scattering of energetic γ-rays made in cosmic ray interactions. These tend to have a relatively flat energy distribution. Thus intrinsically signal/noise deteriorates with increasing energy. Furthermore, it becomes increasingly difficult to shield against the higher energy photons, since compton scattering, which does not remove the photon but simply degrades it in energy, becomes the dominant form of interaction. The technique of active shielding used by Haymes and by Peterson is effective in reducing background.

C. SOFT X-RAY DETECTION TECHNIQUES

The importance of detecting photons with energies below 1 keV is more than simply

https://doi.org/10.1017/S0074180900003971 Published online by Cambridge University Press

the increasing number of photons present at these energies. It may be important to see the low-energy behavior of the X-ray sources. This is best illustrated by the diffuse X-ray background which seems to show an anomalously high intensity at low energy. It is important to establish the number-temperature (power law index) distribution of the sources; i.e., many new sources may be revealed at the very low energies. Finally, the absorbing properties of the interstellar medium and the sources themselves will be revealed at low energies.

In the last few years, a number of experimental groups have concentrated their efforts toward performing measurements below 1 keV using photo-electron detectors and thin-window proportional counters and experiments utilizing the latter devices have achieved some notable results. Physically, the thin-window proportional counters are the same as the beryllium window proportional counter discussed earlier except

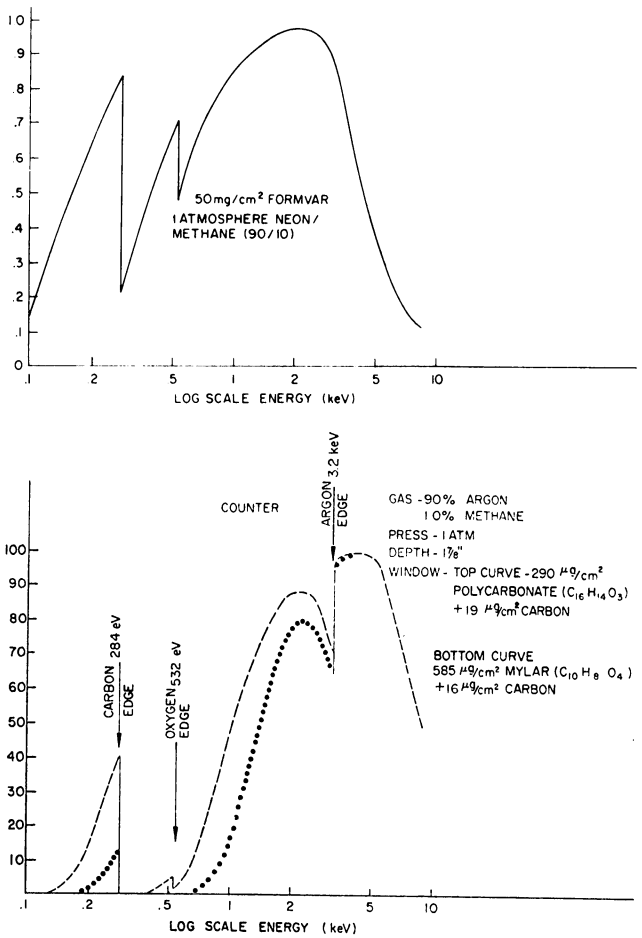

Fig. 5. Calculated efficiency of thin window proportional counters currently being used in sounding rocket experiments.

https://doi.org/10.1017/S0074180900003971 Published online by Cambridge University Press

for the use of the thinner aperture window. Window material that has been used includes 6 and 4μ Mylar, 2μ 'Kimfoil' and Formvar (0.5–1μ). The Lockheed group was the first to attempt flying these detectors. The work of Bowyer *et al.* [4] on the X-ray background was performed using the thinner Mylar, as was the work of the NRL group [7]. Recent results of the Calgary group [8] have been based on the use of 6μ Mylar. Livermore Radiation Laboratory has successfully flown Formvar window detectors and the University of Wisconsin group has flown 'Kimfoil' and Mylar window detectors. The calculated efficiency of the latter's detectors is shown in Figure 5 (lower half) and the efficiency of the Formvar counters flown by LRL in Figure 5 (upper half).

The great advantage of these detectors over the thicker window devices is the response below the carbon edge at 0.28 keV. However, the experimental problems associated with their use are severe. The windows are porous and a gas-ballast or flow system must be used to maintain pressure during the flight. Since the pulse amplitude is a very sensitive function of the gas pressure, the system must be well regulated and a means must be provided to monitor accurately the gas gain of the counter. Also because of the porosity contaminants, principally oxygen and water vapor, can leak in and the detectors must be carefully flushed before flight or kept evacuated until flight.

Finally, there is apparently more difficulty with spurious effects at these very low energies than in the 1–10 keV energy range. The LRL group reports interference from solar induced X-ray fluorescence in the atmosphere on one occasion and from unexplained sources (probably low energy electrons) on another occasion.

As might not be unexpected the experimental results obtained in this area are not entirely self-consistent. Table III lists the published results of measurements at 0.28 of the diffuse X-ray background. The difference between Bowyer *et al.* [4] and Henry

TABLE III

Comparisons of results of measurements of isotropic background at 0.27 KeV

	Reported flux (keV/cm^2-sec-ster (keV))	
	Uncorrected for interstellar attenuation	Corrected
Bowyer *et al.*	65	73
Henry *et al.*	168	790
Baxter *et al.*	583	–

et al. [7] lies mostly in the choice of the interstellar absorption factor. The result of Baxter *et al.* [8] must be regarded with suspicion, not only because it is larger than the other two, but also because the authors do not observe the expected reduction in intensity at low galactic latitude caused by interstellar absorption. The various measurements on the low energy X-rays from Sco X-1 show even greater inconsistencies.

4. Modulation Collimators

Conventional slat collimators can practically be built to provide $\sim\frac{1}{2}^\circ$ collimator. The modulation or wire-grid collimator on the other hand has been successfully used to much smaller angular widths. The device was invented by Oda [9] and was utilized by the AS&E/MIT collaboration to determine the angular size and position of the Crab Nebula and Sco X-1 with very high precision.

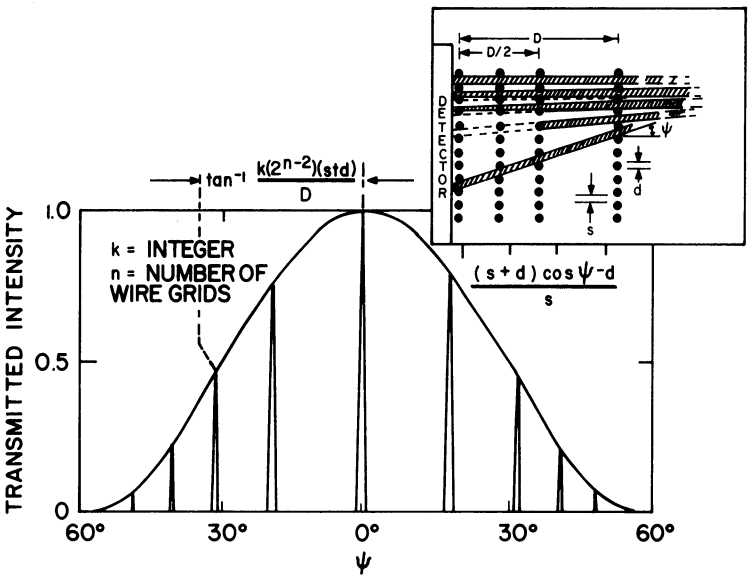

Fig. 6. Angular response of a four grid modulation collimator.

The functioning of the modulation collimator is shown in Figure 6. The use of wires or electro-formed grids allows obtaining the very fine angular resolution. The planes of wires permit X-rays to arrive at the detector from regularly spaced bands in the sky. The angular width of each band is given by the ratio of the separation of the individual wires and the distances between the outermost wire planes. In the case of the Sco X-1, Crab experiment the wire separation was 0.005″ and the overall length of the collimator was 24″ yielding a basic angular resolution of 2×10^{-4} radians or 40 arc seconds. Data obtained by Gursky *et al.* [10] during the traversal of Sco X-1 is shown in Figure 7.

The modulation collimator can be used in a variety of ways as has been discussed by Bradt *et al.* [11]. A novel application of the device as a 'spatial filter' has been discussed by Schnopper *et al.* [12].

5. Sensitivity for Detection of Faint Sources

The sensitivity of an X-ray astronomy experiment for the detection of faint X-ray

https://doi.org/10.1017/S0074180900003971 Published online by Cambridge University Press

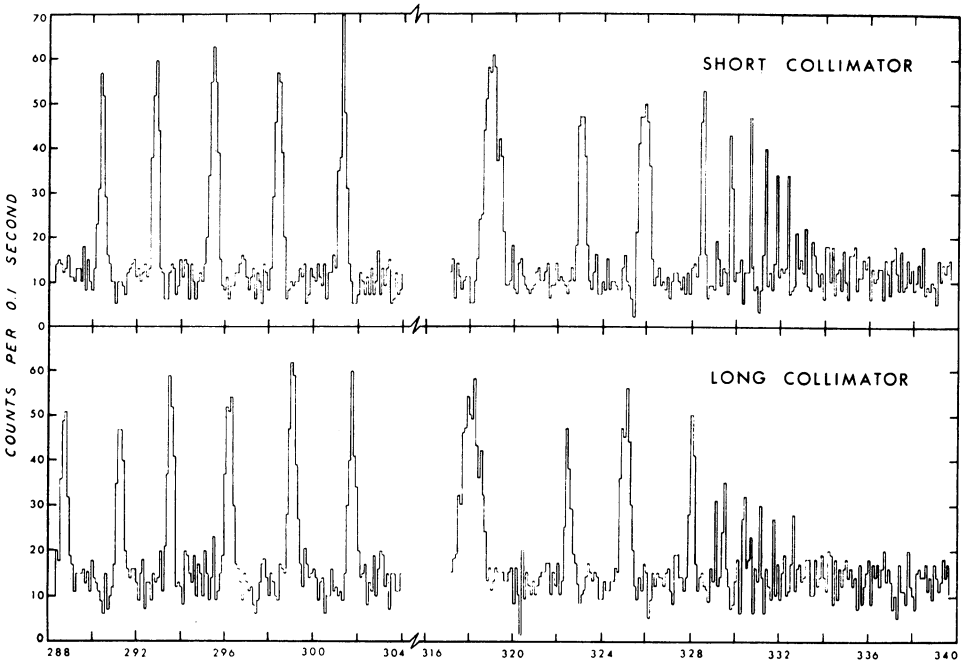

Fig. 7. Response of a four grid modulation collimator to Sco X-1. Data obtained by Gursky *et al.* [10] during the sounding rocket flight of March 1966. Variations in the width and separation of individual peaks related to the varying drift rate of the rocket.

sources is calculated in this section. The calculation is quite general and can be applied to any scanning type of experiment. The only precaution is that background rates will, of course, be very dependent on the energy range being considered.

The accumulated count N including non-source counts from a source of intensity, I, is given by

$$N = (fI + \Omega B_1 + B_2)\, At \text{ counts} \tag{1}$$

where t, the actual observing time on a source, is given by either

$$t = (\xi/2\pi)\, T \text{ continuously rotating vehicle.} \tag{2}$$

$$t = \xi/\dot{\xi} \text{ single slow scan.} \tag{3}$$

T is the total observation time, ξ is the field of view in the direction of the scan, and $\dot{\xi}$ is the scan rate.

The other quantities in Equation (1) are as follows: f = vignetting factor (0.75 for mechanical collimators, if ξ is taken to be FWHM); Ω = total field of view (ster); B_1 = diffuse X-ray background (counts/cm^2-sec) (Ster)); B_2 = non-X-ray background (counts/cm^2-sec); and A = effective detector area.

Both B_1 and I can be obtained from more basic quantities from the following

https://doi.org/10.1017/S0074180900003971 Published online by Cambridge University Press

relation

$$I = \int_{E_1}^{E_2} \varepsilon(E)\,(\mathrm{d}\phi/\mathrm{d}E)\,\mathrm{d}E \text{ counts/cm}^2\text{-sec} \tag{4}$$

where $\mathrm{d}\phi/\mathrm{d}E$ = spectral distribution of the X-radiation (photons/cm^2-sec (keV)), and $\varepsilon(E)$ = efficiency of detection as a function of energy E.

The efficiency for proportional counter in turn is calculated from the relation

$$\varepsilon(E) = \exp(-\mu_w x_w)\,[1 - \exp(\mu_g x_g)] \tag{5}$$

where μ = mass absorption coefficient of the detector window (μ_w) or gas (μ_g), and x = thickness (gm/cm^2) of the window (x_w) or gas (x_g).

Equation (4) is only approximate in that it gives the number of photons converting in the detector, but not the number of recorded counts. To obtain the latter one must take into account the details of the response of the detector, principally, the energy resolution and the escape of fluorescent radiation.

The maximum sensitivity is arrived at by the following recipe. In the first place, we assume I is much smaller than $\Omega B_1 + B_2$. Secondly, we state that the weakest observable source is one that gives a number of counts (N_m) equivalent to a 3σ fluctuation of the accumulated count when no source is present.

Thus

$$\begin{aligned} N_m = f I_m A t &= 3\sqrt{N} \\ &= 3\sqrt{(\Omega B_1 + B_2)\,At} \end{aligned} \tag{6}$$

or

$$I_m = (3/f)\sqrt{(\Omega B_1 + B_2)/At}.$$

Listed in Table IV are values of At appropriate to particular kinds of experiments and the corresponding minimum observable fluxes. B_1 is taken to be ~ 5 cts/cm^2-sec (ster). The values of B_2 were taken appropriate to experiments performed in the 1–10 keV energy range near the earth's equator, where the effects due to cosmic rays are mini-

TABLE IV

Minimum sensitivity for various experiments

	At(cm^{-2}-sec^{-1})	I_m(counts/cm^2-sec)	In relation to Crab
Recent AS & E Sounding Rocket Experiments (80 sq. deg.)	8000	1.5×10^{-2}	10^{-2}
Ultimate Sounding Rocket ($\Omega B_1 \ll B_2$)	10^5	10^{-3}	5×10^{-4}
X-ray Explorer (1 day, 25 sq. deg.)	4×10^5	10^{-3}	5×10^{-4}
X-ray Explorer (1 week, 25 sq. deg.)	3×10^6	4×10^{-4}	2×10^{-4}
Super Explorer (10 m^2, 1 hr. integration) ($\Omega B_1 \ll B_2$)	2×10^8	3×10^{-5}	1.5×10^{-5}

https://doi.org/10.1017/S0074180900003971 Published online by Cambridge University Press

mized. The condition $\Omega B_1 \ll B_2$ is satisfied for Ω the order of several square degrees. The X-ray Explorer is a payload being prepared for flight in 1970. It will be described in Section 7. The Super Explorer is a payload now in the planning stage at NASA.

The sensitivities presented in Table IV must be examined critically, however, since even the 'ultimate' sensitivity achievable with a sounding rocket has not nearly been achieved. In the case of the sounding rocket, the assumption is that one does a simple on-source, off-source type of scan, which is also the assumption in the case of the Super Explorer example. In the latter case the observing time is taken to be 1 hour. The difficulty with both of these two cases is that they are not suitable for scanning large regions of the sky. They can only be used to sample the sky, or to look at regions of especial interest; otherwise, the total time requirements become prohibitive. This situation occurs as well with major radio and optical observatories; namely, that the ultimate sensitivity of the largest aperture instruments is achieved in only a very limited class of observations. A good example of this is the observation of the radio emission from Sco X-1 by Ables [13], in which at least one order of magnitude greater sensitivity was achieved than is usual for surveys with radio telescopes.

The basic conclusion is that very great improvements in sensitivity can be achieved with conventional instruments, approaching the 10^{-5}–$10^{-6} \times$ Crab discussed earlier.

6. Measurements of Source Characteristics

A. LOCATIONS

A single traversal of a source with a mechanical collimator yields a counting rate profile that is typically triangular in shape. The width of the triangle is determined by the collimator and can be as narrow as $\sim\frac{1}{2}^\circ$ for conventional, slat collimators, or as little as a fraction of an arc minute for a wire-grid collimator. The position of the centroid of the counting rate profile determines the X-ray source location to a line on the sky and repeated traversals with varying collimator orientations can be used to obtain intersecting lines of position to further pinpoint the location of source as is shown in Figure 8, which is based on data obtained from a scan of the Cygnus region. Alternately, one can build up count-rate distribution on the sky and find the centroid of that distribution. The precision with which locations can be determined is directly related to the half-width of the collimator and the strength of the source. Also, since it is not possible to reference one X-ray source location to that of other known X-ray sources, it is necessary to determine independently the orientation of the collimators with respect to the star-field.

B. SPECTRAL DATA

The use of proportional counters and scintillation counters allows obtaining spectral data by analyzing the amplitude distribution of the counter signals; essentially, by unfolding the counter response from the amplitude distribution. The technique is described in detail by Gorenstein *et al.* [11a]. The principal complicating factor in these analyses is the fact that not all the energy of an X-rays interacting in the gas of a

proportional counter (or in a scintillation crystal) is necessarily deposited in the counter. Secondary fluorescence radiation can escape from the counter and the resulting signals have a lower than expected amplitude.

Spectra obtained in the 1–10 keV can be resolved to between 20 and 30%. At low

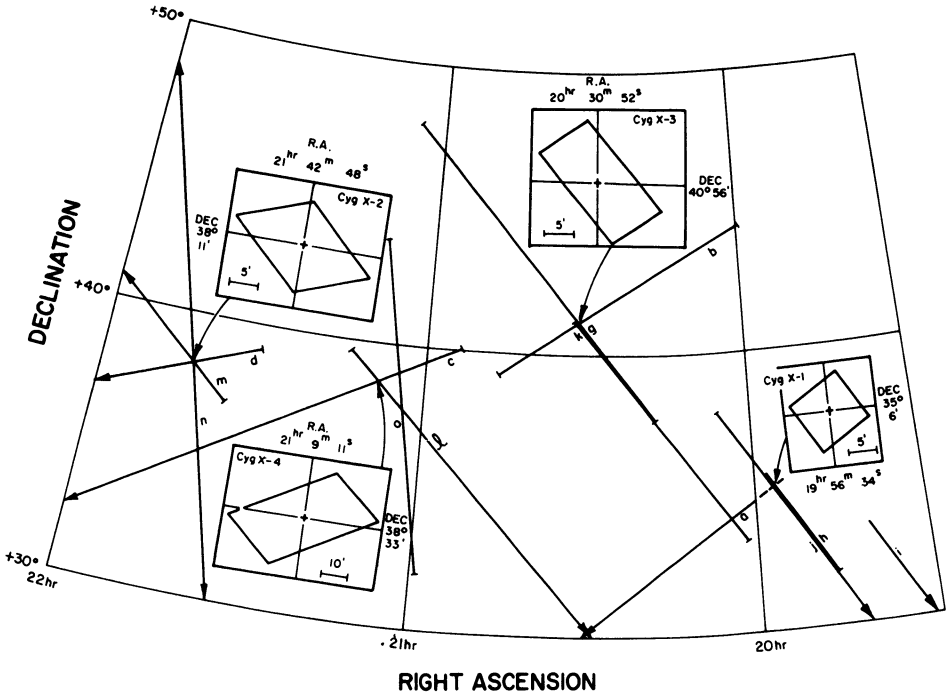

Fig. 8. Location of X-ray sources in Cygnus based on sounding rocket flight of November 1967. Individual lines of positions *a* through *o* are obtained from centroids of peaks in the counting rate curve.

energy, spectral data are best obtained by filter techniques. The presence of absorption edges allows high transmission only below the energy of the edge. The filter can be just the counter window. The very soft X-ray detectors all make use of the carbon edge to obtain spectral data at 0.28 keV. Other counters have been constructed that make use of the aluminum edge at 1.5 keV and the fluorine edge (teflon) at 0.7 keV.

Although spectral data have been used almost exclusively to determine the shape of the energy distribution, it should be possible to detect at least one spectral line, if it is present, namely, the iron line at 7.1 keV. Tucker [14] has calculated that the emission in this line should constitute about 1% of the total X-ray emission from a hot plasma of 5×10^7 K temperature with the normal abundance of iron. This feature has been searched for unsuccessfully in Sco X-1 by Fritz *et al.* [15] during an observation with an exposure (At) of 4000 cm^2-sec. The authors estimated that an exposure of at least 16000 cm^2-sec was required to observe the iron line strength predicted by Tucker. Such exposures are well within the capabilities of sounding rocket experiments.

https://doi.org/10.1017/S0074180900003971 Published online by Cambridge University Press

C. POLARIZATION

Novick and his collaborators have searched for polarization of the X-rays from Sco X-1 and from the Crab Nebula using a Thompson scattering polarimeter [16]. The technique involves allowing the X-rays to be incident on blocks of lithium and detecting the X-rays scattered at right angles. Because of the competition between photo-absorption and scattering, the sensitivity of such a polarimeter peaks at about 7 keV. The result on Sco X-1 was that the source was unpolarized to a 1σ limit of 7%, for an exposure of about 10^5 cm^2-sec. The actual area was 900 cm^2 and represents the geometric area of the entire instrument. In order to obtain a significant result on the Crab an exposure of about 10^6–10^7 cm^2-sec with this instrument is required. It may be possible to construct a more efficient polarimeter using hydrogen as the scatterer.

7. Description of the X-Ray Explorer

Rather than describe additional elements of X-ray instrumentation individually, I want to describe an entire experiment; namely, the X-ray Explorer Payload which is being prepared by AS&E under NASA sponsorship for flight in 1970. The payload is essentially similar to sounding rocket payloads that we and others have flown. This experiment is the first of NASA's small astronomy satellites (SAS). The second

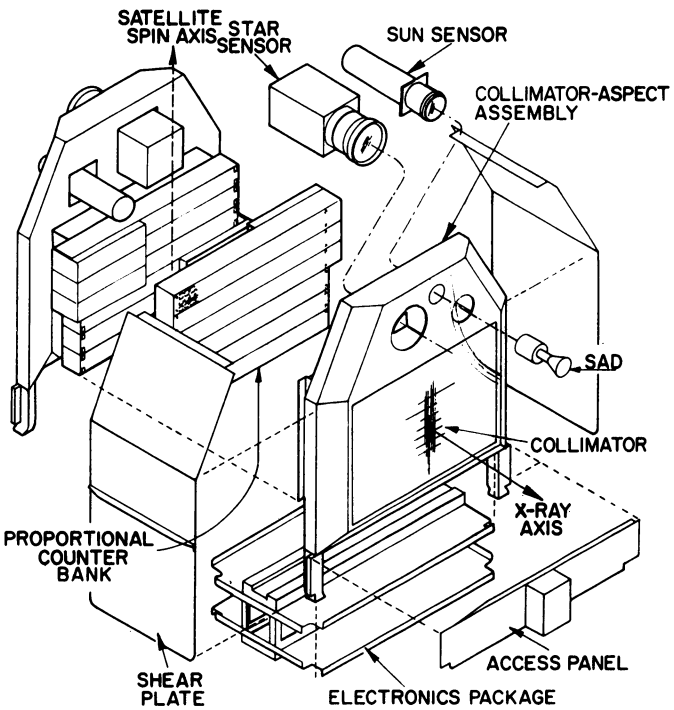

Fig. 9. Exploded view of the experiment portion of the X-ray Explorer satellite.

https://doi.org/10.1017/S0074180900003971 Published online by Cambridge University Press

SAS payload is to be devoted to γ-ray astronomy using a spark chamber. Later SAS payloads will be pointed and are planned for both X-ray astronomy and optical astronomy.

The principal scientific objective of the Explorer mission is an all-sky survey to a limit of sensitivity of about $10^{-3} \times$ Crab in the energy range 1–10 keV. Spectral data are obtained by the use of proportional counters. Positional accuracy of source locations will be $\sim 1'$ for the stronger sources. Time variations can be studied on a time scale of minutes, days and months and the useful life of the satellite should be at one year.

The payload is shown schematically in Figure 9. The unit is organized into two, almost identical halves. The collimators are built up from extruded aluminum tubing. The field of view on one side $\frac{1}{2} \times 5°$ (FWHM) and the other side is $5° \times 5°$. The detectors on both sides are beryllium window proportional counters. The window thickness is 2 mils (50μ). The effective area on each side is about 800 cm^2. Attitude is determined by a star sensor – sun sensor combination.

The spacecraft portion is being built by the Applied Physics Laboratory of Johns Hopkins University. Its basic characteristics are as follows. The spacecraft is spin-stabilized by a high-speed rotor, the spacecraft itself will spin with about a 10 min period, which will be controllable. The spin axis can be pointed to any position in

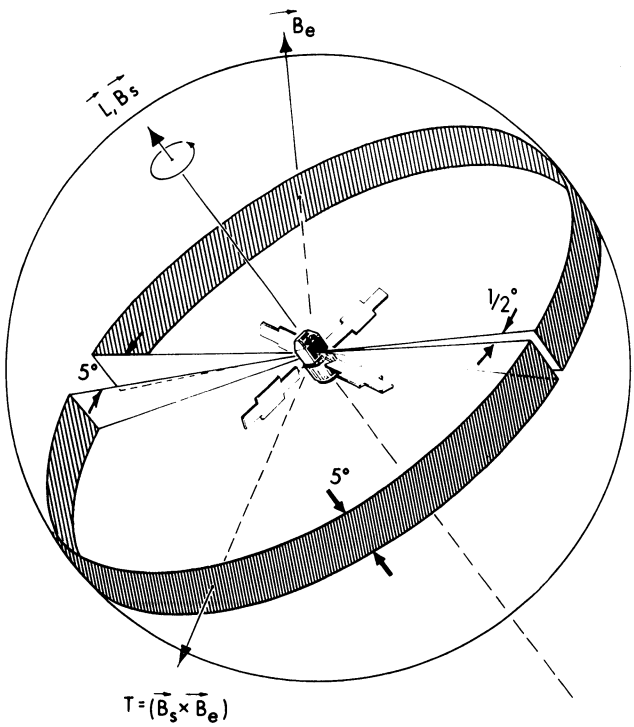

Fig. 10. Scan and maneuver geometry for the X-ray Explorer on the celestial sphere. Maneuvring is performed by internally generating the magnetic field B_s along the spacecraft spin axis which interacts with the earth's magnetic field B_e to produce the Torque T as shown.

https://doi.org/10.1017/S0074180900003971 Published online by Cambridge University Press

the sky using a magnetic torqueing control. As shown in Figure 10 the X-ray detectors will sweep out a 5° band in the sky once per rotation. We plan to spend between $\frac{1}{2}$ and one day per band and then reposition the spin axis to scan out another band. At this rate about a month will be required to scan the entire celestial sphere.

As shown in Table IV, the ultimate limit of sensitivity of the Explorer payload could be about $10^{-4} \times$ Crab. Based then on the extrapolation of source distributions shown in Table II, as many as $\sim 10^3$ sources could be observed compared to the 40 or so now reported. Of course many of these, particularly in the Sgr-Sco region will not be resolved.

In addition to an all-sky survey, the maneuvring capability and the extended lifetime of the Explorer spacecraft allows operating the experiment in a manner analogous to that of a conventional astronomical observatory. Observations can be planned according to a pre-arranged schedule to allow simultaneous acquisition by other groups of optical or radio data. Individual experiments can be planned that call for extended periods of time observing a single source or particular region of the sky and certain transient phenomena (such as novae outbursts) can be investigated for accompanying X-ray emission.

8. Grazing Incidence Optics

I have discussed above certain limitations of 'conventional' X-ray instrumentation; notably, the difficulty of working at long wavelengths and the restriction on angular resolution. Instruments that employ grazing incidence optics do not suffer from these limitations and, additionally, offer the possibility of very high sensitivity for the detection of faint sources, high spectral resolution, and efficient polarimetry. Above all, telescopes allow obtaining pictures in X-rays of cosmic features such as the Crab Nebula, Cas A and M-87 and more ambitiously of M-31. Such pictures have been obtained of the sun by the Solar Physics Groups at American Science and Engineering and the Goddard Space Flight Center.

The fact that X-rays reflect at grazing incidence allows the construction of focussing optics. This was first discussed by Wolter [17] in connection with X-ray microscopy and astronomical applications were proposed by Giacconi and Rossi [18]. Functioning telescopes were first developed at AS & E and their initial application was solar photography.

X-ray optics can be used in a variety of configurations, as shown in Figure 11. The only configuration which I will discuss in detail will be the two-surface focussing arrangement of paraboloid-hyperboloid. This is not to say that the other configurations may not find important applications in certain circumstances, it is rather that this one has the widest range of applications and imposes a minimum of operational restraints.

The most important single parameter characterizing the device is the grazing angle (α) for paraxial radiation on the first surface. The wavelength response, the collecting area and the focal length are determined by this quantity. The calculated reflectivity

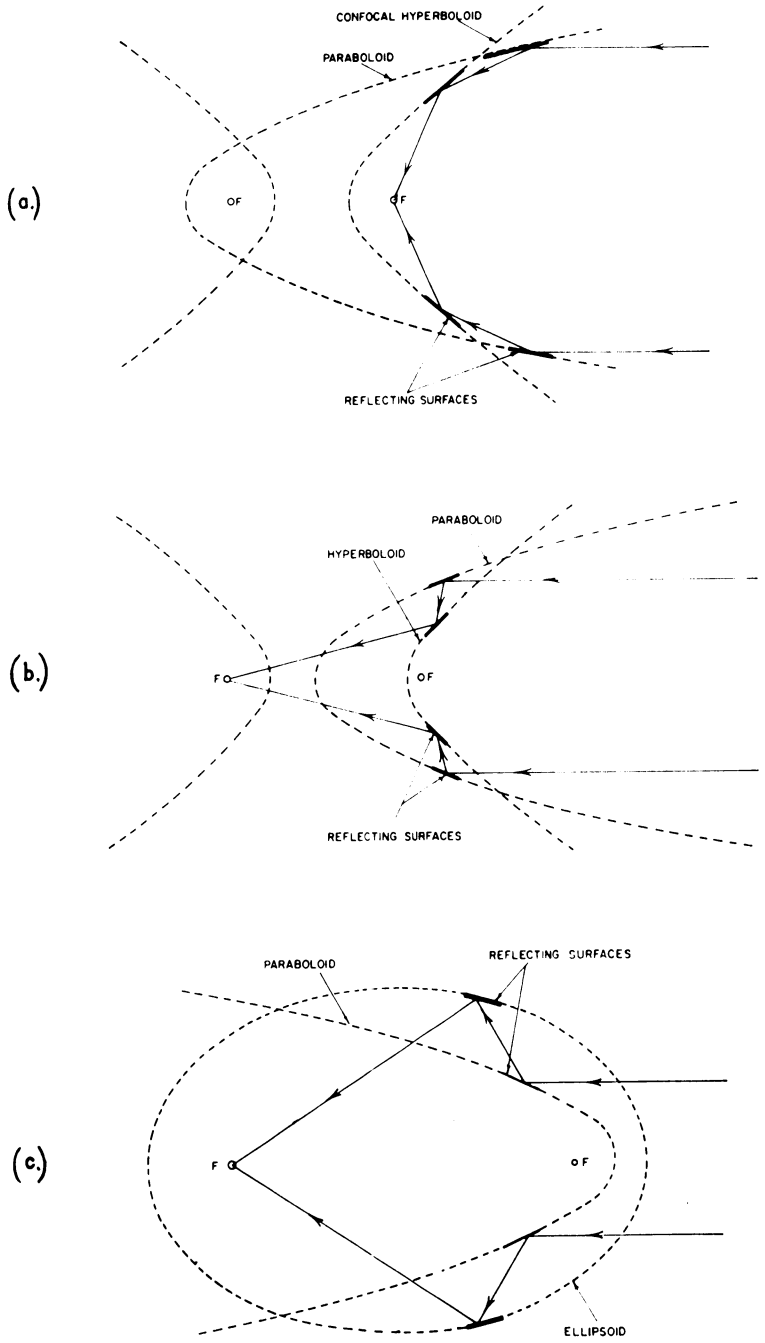

Fig. 11. Three possible configurations of reflecting services that can be used for producing X-ray energies.

https://doi.org/10.1017/S0074180900003971 Published online by Cambridge University Press

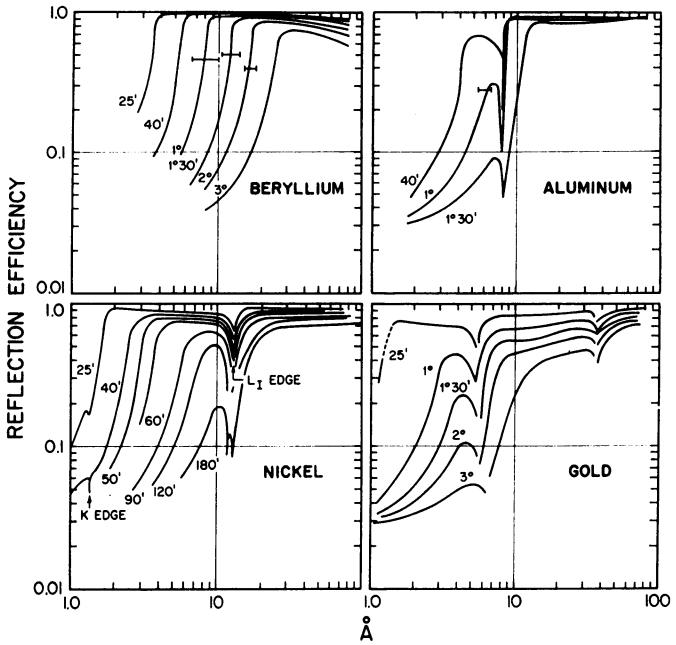

Fig. 12. Calculated reflectivity for several materials at grazing angles of incidence.

TABLE V

Telescope parameters

	Telescope A[a]	Telescope *B*[a]
Diameter (cm)	30.5	87
Focal length (meters)	2.1	6.1
Collecting area (cm^2)	44	1000
Field of view, diameter (degrees)	1	1
Point-source image distribution	5% of incident flux imaged in 5 arc sec diameter circle	20% of incident flux imaged in 2 arc sec diameter circle
Telescope resolution element (maximum size)	5 arc sec	2 arc sec
Net effective area in tel. resolution element (cm^2)[b]	0.22	20
Noise/telescope resolution element (counts/sec)	10^{-3}	10^{-3}
Number of telescope resolution elements in field	5×10^5	3×10^6

[a] The mirrors of Telescope A are identical to those which have been fabricated for the S-054 solar X-ray telescope experiment to be flown on the NASA Apollo Telescope Mount. Telescope B is a system we are designing for a stellar X-ray astronomy experimental program.
[b] Calculated on the basis of a detector efficiency of 10%.

https://doi.org/10.1017/S0074180900003971 Published online by Cambridge University Press

for several materials is shown in Figure 12. One sees the characteristic cut off at short wavelength and the discontinuities at the absorption edges.

Other properties of a telescope are derived (approximately) from the following relations:

Collecting area $A=\pi R^2 l\alpha$

Focal length $f=R/8\alpha$

where R=radius of aperture and l=length of mirror section. The field of view of the telescope is approximately α.

The specifications of mirrors that are being planned for flight use are listed in Table V.

In principle very high angular resolution can be attained with X-ray telescopes. Even for the smallest aperture devices yet built the diffraction limit is less than 0.01″. More practical limits are imposed by mechanical tolerances and surface finish. The results of a ray tracing study are shown in Figure 13, which indicates that a fraction of an arc second resolution can be achieved within the central arc minute of a 'real' telescope; by real I mean one that is figured to state of the arc tolerances. Resolution

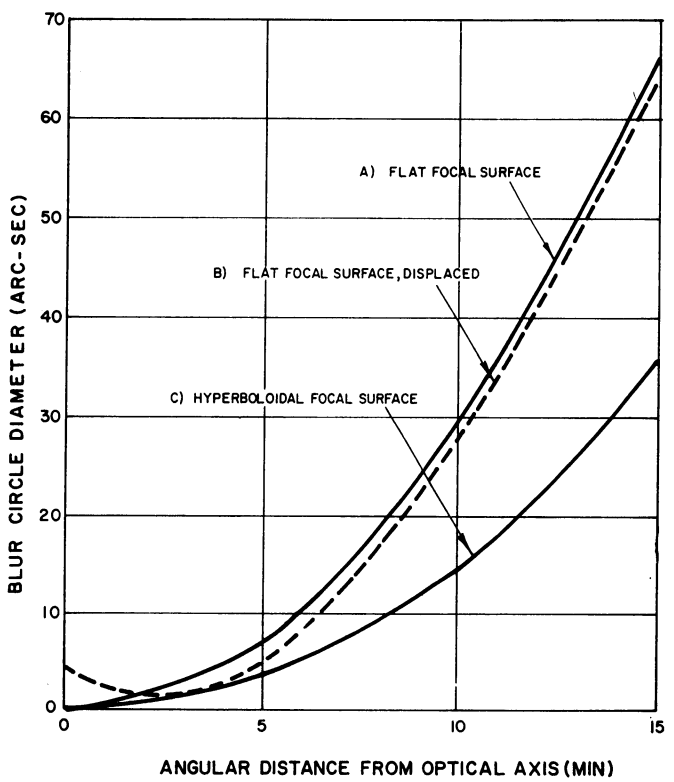

Fig. 13. Blur circle diameter vs. angular distance for the optical axis of a paraboloid-hyperboloid telescope as obtained by the ray drawing analysis.

https://doi.org/10.1017/S0074180900003971 Published online by Cambridge University Press

of several arc seconds has been achieved in AS & E sounding rocket flights [19], as is shown in Figure 14. Examples of existing telescopes are shown in Figure 15.

In comparison to the angular resolution, only poor efficiency (reflectivity of the surfaces) has been obtained with present telescopes. The telescope used to obtain the picture in Figure 14 had a net reflectivity of only several percent or about a factor of 10 below the calculated value. This is apparently the result of diffuse scattering from surface irregularities. The present AS & E mirrors have been fabricated by Diffraction Limited from Kanigen (an amorphous nickel alloy) which is coated onto beryllium. The surface finish is good only to between 50–100 Å. It is anticipated that more satisfactory performance can be obtained with materials such as cervite or fused silica

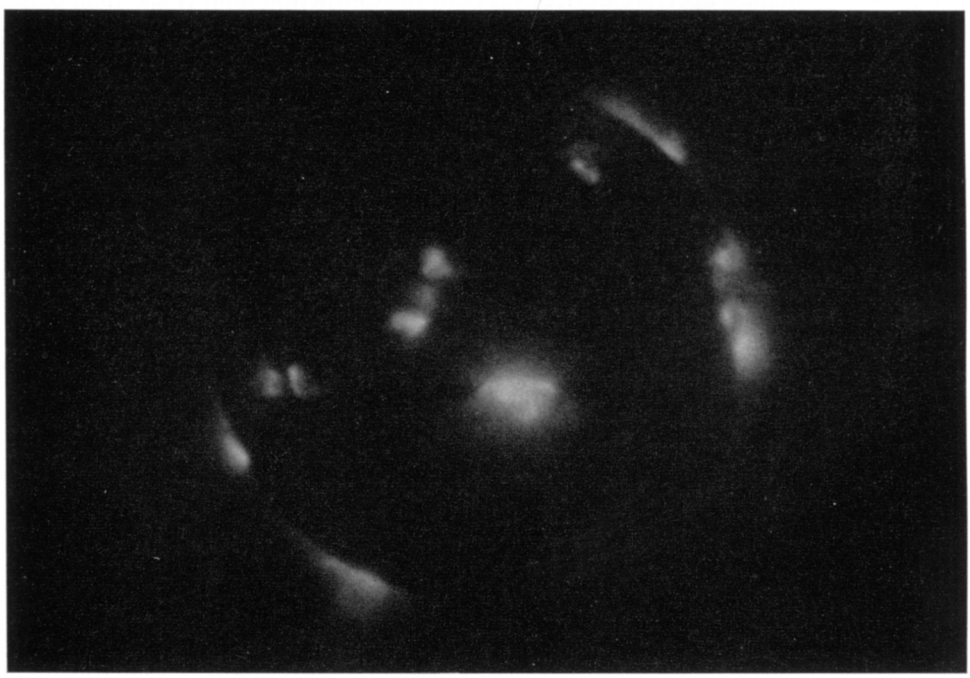

Fig. 14. X-ray photograph of the sun obtained on June 8, 1968, by the AS & E Solar Physics group using a 9″ diameter telescope. The rocket was flown during a solar flare which shows up as the very bright region near the center of the picture.

which is known to take a superior finish compared to Kanigen. Fused silica telescopes have been successfully flown by the Solar Physics group at Goddard Space Flight Center [20].

Fig. 15. Existing X-ray telescopes. The top figure shows the sounding rocket telescope used to obtain the photograph in Figure 14; the bottom photograph illustrates a pair of confocal, axial telescopes that will comprise the mirrow system for AS & E solar ATM experiment. →

https://doi.org/10.1017/S0074180900003971 Published online by Cambridge University Press

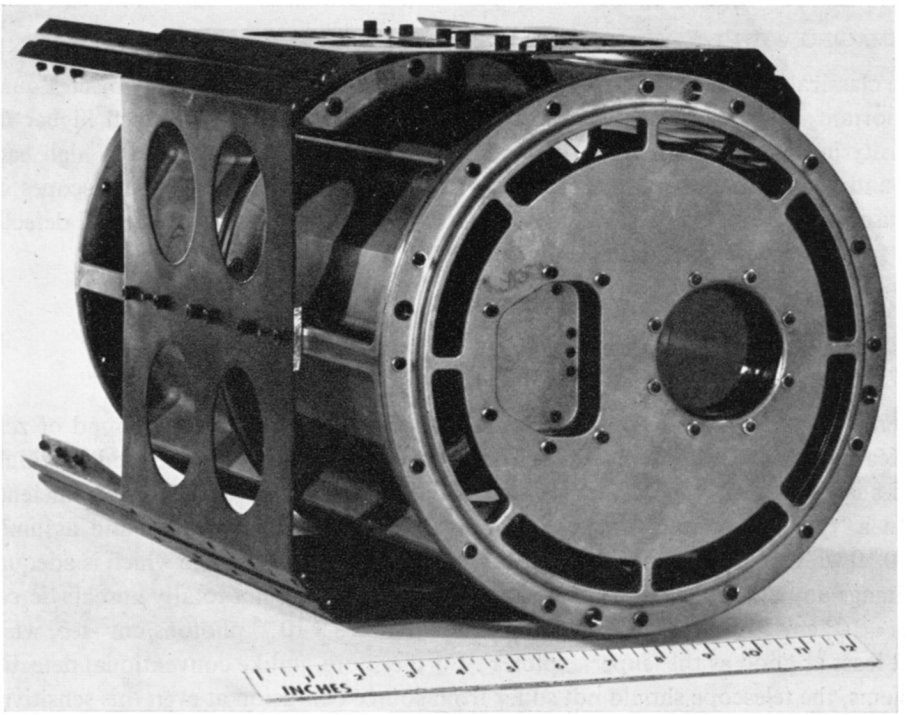

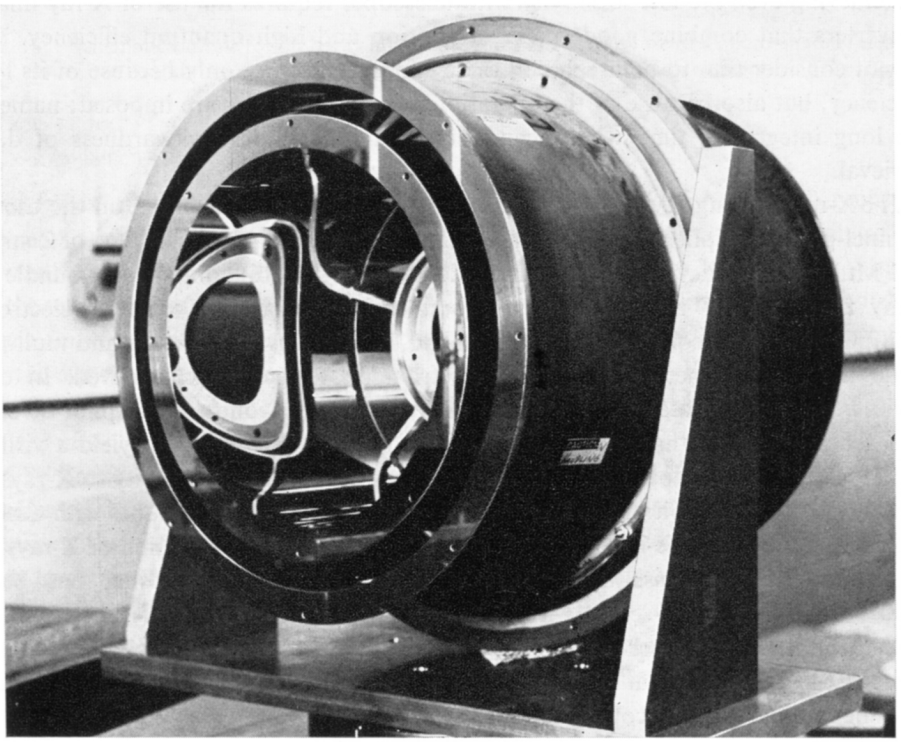

https://doi.org/10.1017/S0074180900003971 Published online by Cambridge University Press

A. IMAGING WITH X-RAY TELESCOPES

The classical use of a telescope is, of course, to produce an image of an object. Equally important is the fact that telescopes concentrate; i.e., produce a much higher flux density in the focal plane than is present at the aperture. In view of the high background of X-radiation that is present, this concentration means that telescopes can be used to achieve very high sensitivity. Assuming that one has a 'noiseless' detector, the faintest observable source is one yielding a flux, Φ min, given by,

$$N_n = 10 = \varepsilon A T \Phi_n \text{ counts}$$

or

$$\Phi_n = 10/\varepsilon A T \text{ photons/cm}^2\text{-sec},$$

where 10 counts is taken to be the minimum signal (against a background of zero) indicating the presence of a source. The quantities A and T are as defined previously and ε is the net throughput, including the mirror reflectivity and detector efficiency.

In a 'typical' sounding rocket experiment $A = 40\text{ cm}^2$, $T = 250$ sec and assuming $\varepsilon = 0.10$ which should be achievable, Φ min $\simeq 10^{-2}$ photons/cm^2-sec which is adequate to image any of the known sources. A more ambitious, but not totally unrealistic case is $A = 10^3$ cm^2, $T = 3600$ sec, in which case Φ min $\simeq 3 \times 10^{-5}$ photons/cm^2-sec, which is at least as good as the 'super-explorer'. Furthermore, unlike conventional detection systems, the telescope should not suffer from source confusion at even this sensitivity.

Achieving even modest sensitivity with telescopes requires the use of X-ray image converters that combine good spatial resolution and high quantum efficiency. We do not consider film to be useable in these experiments; not only because of its low efficiency, but also because of the operational constraints that are imposed; namely, the long integrating time while accurately pointed and the awkwardness of data retrieval.

The X-ray imaging device that AS & E has been developing is based on the use of channel-plate multipliers as have been developed by Bendix, Rauland (Div. of Zenith) and Mullard. This device (shown schematically in Figure 16) consists of a bundle of many thousands of individual glass tubes, each comprising a channel electron-multiplier. Photons, converting at the front end, continuously accelerate and multiply down the tube. A net gain of $\sim 10^5$ electrons/photoelectron is achieved. In our devices, the output electrons are additionally accelerated onto a phosphor screen. The net gain is such that each X-ray converted at the front end will yield a visible (or photographable) spot of light on the phosphor screen. The sensitivity to X-rays is achieved by coating a bit of the inner surface of the front end of the tubes with CsI or similar material which is known to have a high efficiency for conversion of X-rays to photoelectrons. The noise in devices which AS & E has been using has been $\sim 10^{-3}$ counts/res. elem-sec and it is not known whether this figure represents any kind of limit. The number is the basis for our statement about noiseless detectors; namely, for an image that occupies a single resolution element, the 'noise' would amount to only a single 'count' in 1000 sec.

https://doi.org/10.1017/S0074180900003971 Published online by Cambridge University Press

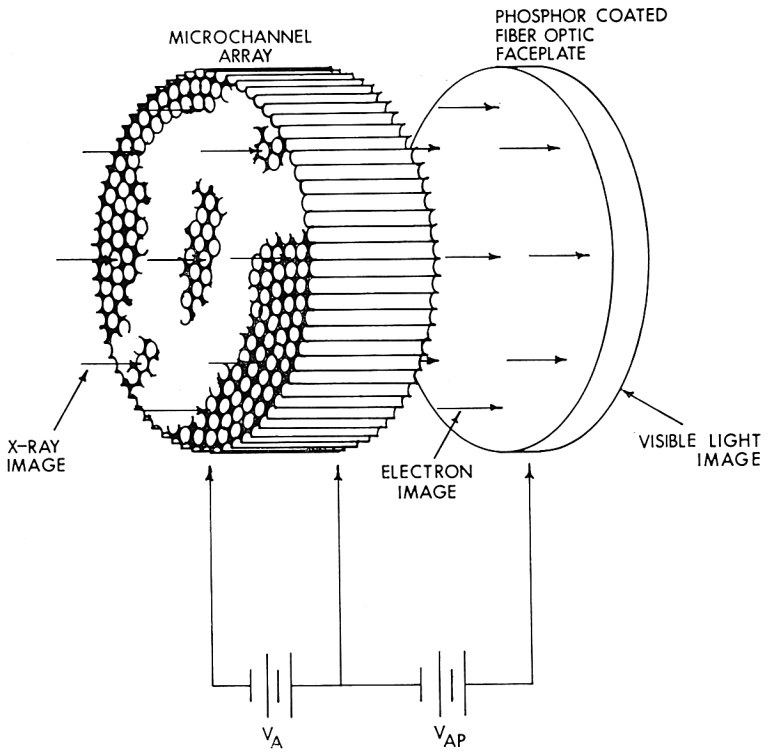

Fig. 16. Schematic outline for an X-ray image intensifier that makes use of a micro-channel electron multiplier array. Each channel defines a single resolution element.

B. X-RAY SPECTROSCOPY

Two kinds of dispersing spectrometers have been proposed for use with focussing telescopes; one, which has been studied by Schnopper and Kalata [21] makes use of a curved Bragg Crystal in a Johann Mount, as shown in Figure 17. The X-ray image of the telescope is placed on the Rowland circle and forms a line-image on the Rowland circle for X-rays satisfying the Bragg condition. The choice of crystal is determined by the wavelength to be studied. Mica with a 2d spacing of 13 Å and KAP with a 2d spacing of 26.4 Å are typical choices. With these spectrometers, resolution of $(\lambda/\Delta\lambda)$ of $\sim 10^3$ is attainable.

The Bragg spectrometer can be used without a telescope as is commonly done in studies of the sun, in which case a flat crystal is used. There are two principle difficulties with this geometries; namely, since the crystal face constitutes the aperture, very large apertures may be difficult to attain, and also the detector must be as large as the crystal face and one has a very adverse signal/noise situation since only a very small fraction of the incident beam is transmitted to the detector.

A totally novel dispersing spectrometer has been developed for use in X-ray astronomy, which is the slitless spectrometer as proposed by Gursky and Zehnpfennig

https://doi.org/10.1017/S0074180900003971 Published online by Cambridge University Press

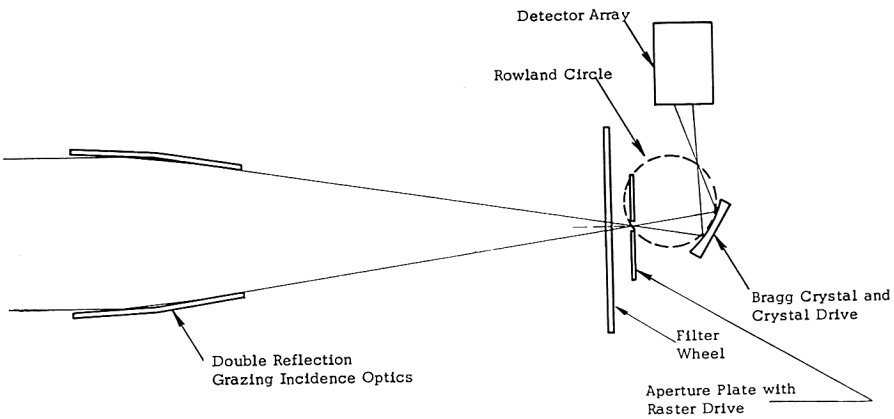

Fig. 17. A focussing high resolution spectroscopy using an X-ray telescope and a spherically bent crystal.

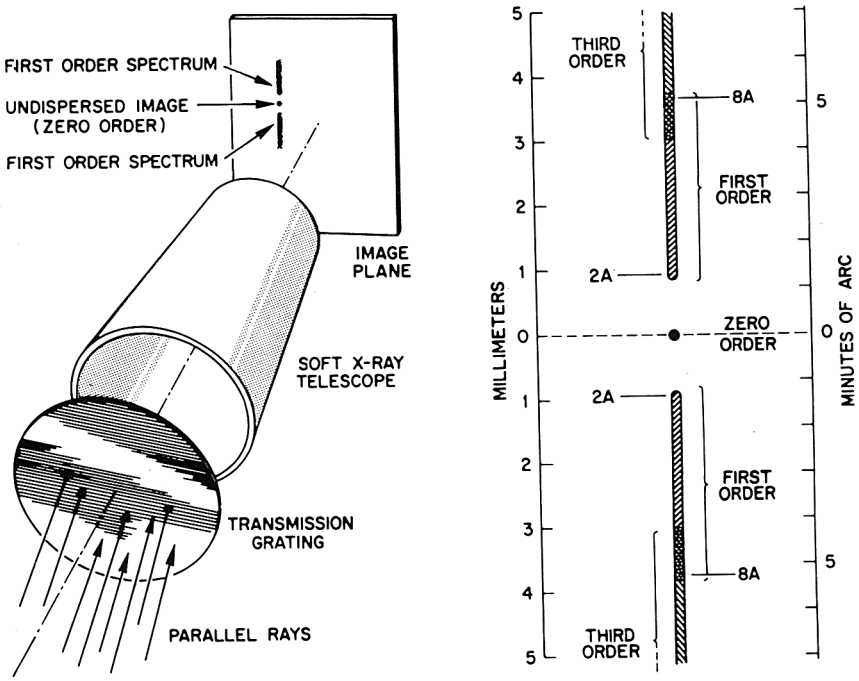

Fig. 18. Schematic representation of the X-ray slitless spectrometer using a transmission grating.

[22]. As shown in Figure 18, a transmission diffraction grating placed behind the telescope mirror, produces a diffracted image in the focal plane. The incident beam is diffracted by the amount

$$\theta = n\lambda/d \quad n = 0, 1, 2, \ldots,$$

where d is the grating spacing. In principle the dispersing power of the spectrometer

https://doi.org/10.1017/S0074180900003971 Published online by Cambridge University Press

is determined by the quality of the grating as H is for any grating spectrometer, in practice, the actual angular dispersions are so small ($\sim$arc minutes) that the angular resolution ($\Delta\theta$) of the mirror determines the dispersing power; i.e.,

$$\lambda/\Delta\lambda \approx \theta/\Delta\theta = n\lambda/d(\Delta\theta).$$

A spectrum obtained with this device is shown in Figure 19. $\lambda/\Delta\lambda$ of 50–100 seems to be attainable.

The Bragg spectrometer and grating spectrometer are totally different instruments

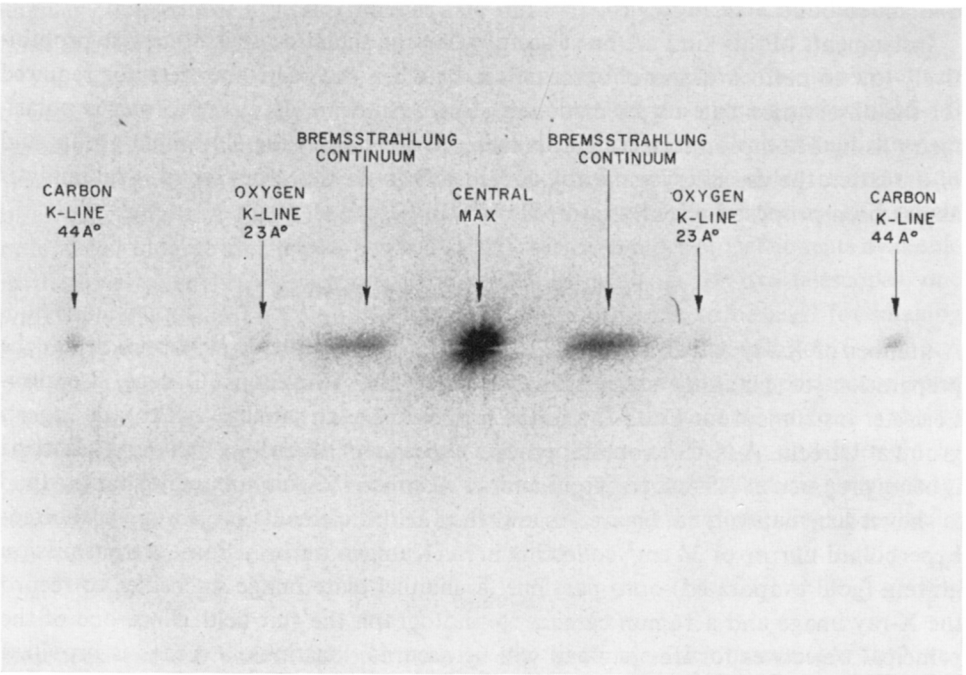

Fig. 19. A spectrum obtained from a thick target bremsstrahlung X-ray source using the slitless spectrometer obtained by Zehnpfennig.

and will be utilized for correspondingly different observations. The Bragg spectrometer is very slow since it is sensitive to only a single wavelength per crystal setting. On the other hand its great resolution allows the possibility of studying line profiles and of observing wavelength shifts as might be caused by doppler or gravitational effects. By comparison the grating spectrometer is a crude device, but does have very high sensitivity since a large fraction of the X-rays ($\sim$40%) is dispersed and the entire spectrum can be studied simultaneously. This device will be most useful for determining the general features of X-ray spectra (line emission, absorption features) for even very faint sources.

C. OTHER APPLICATIONS OF GRAZING-INCIDENCE OPTICS

The ability of X-ray optics to concentrate flux allows development of instruments

https://doi.org/10.1017/S0074180900003971 Published online by Cambridge University Press

that otherwise do not necessarily make use of the imaging properties of the optics. The concentration factor is just the ratio of the effective telescope collecting area to the arc of the detector in the focal plane and can be as large as several thousand. This means that the signal/noise in the detector can be improved by the same amount. Fisher of Lockheed has used an arrangement of focussing slats in this capacity. A more ambitious instrument developed by the Columbia group used microscope slides arranged in a segmented approximation to a two-surface telescope. These arrangements should be particularly useful at low photon energies where large detectors are difficult to build.

Instruments of this kind are most useful when the signal/noise is otherwise prohibitively low to perform a useful observation, or when the particular detector required for the observation can not be made very large. An example of the former is polarimetry using Thompson scattering as is being performed by the Columbia group, and of the latter, the use of cryogenically cooled solid-state detectors for spectral analysis as has been proposed recently by Boldt of GSFC.

10. Description of Telescope Systems

A number of X-ray astronomy experiments that incorporate X-ray optics are in the preparation or planning stage. These include the University College, London-Leicester instrument for OAO-C and the proposed Dutch satellite by Prof. de Jager's group at Utrecht. A NASA sounding rocket experiment that uses a focussing telescope is being prepared at AS & E for flight and an Aerobee 150 this summer. That payload is shown schematically in Figure 20, and the various elements include a paraboloid-hyperboloid mirror of 34 cm^2 collecting area (Kanigen on beryllium), a transmission grating (gold evaporated) onto parylene, a channel-plate image intensifier to record the X-ray image and a 16 mm camera to photograph the star-field. Since one of the principal objectives for this payload will be accurate locations, a means is provided to cross-reference the X-ray image intensifier and the star-field camera. This is accomplished by having an image of the image intensifier appear on the star-field. The

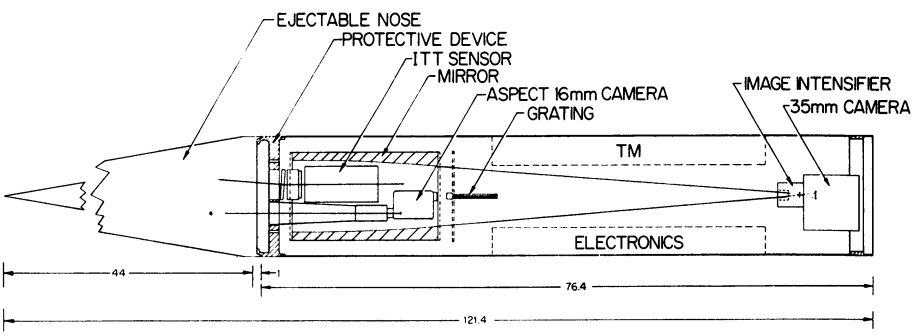

Fig. 20. Layout of a sounding rocket experiment making use of an X-ray telescope for high resolution studies of X-ray sources. This payload is being prepared for flight on an Aerobee 150.

https://doi.org/10.1017/S0074180900003971 Published online by Cambridge University Press

face of the image intensifier will be illuminated and will be viewed through the X-ray telescope by the star camera through a cross-cube prism. This allows direct reference of the X-ray image to the star image.

The sounding rocket group at GSFC is responsible for the remainder of the instrumentation. The guidance system is the stellar-strap, which consists of a gyro-controlled, gas jet course attitude control, and an ITT star-tracker for fine attitude signals. The star-tracker will lock onto a pre-selected bright star ($\leqslant +2.5$ m); since, the X-ray object in general is not coincident with a visually bright object there must be an angular offset between the star-tracker axis and the X-ray optic axis. This system will hold to a target to within $\sim 5''$.

The capability of this payload will be as a slitless spectrometer to obtain a spectrum of Sco X-1, or to image any of the known sources with the possible exception of M-87. As an example of the latter, the recently prepared pulsar in the Crab should show up clearly as a point image within the diffuse nebula, even during the short time duration of a rocket flight. A far more ambitious NASA program calls for the use of a single or a cluster of large area telescopes as a facility with a number of instruments available in the focal plan for observations. One possibility provides for two telescopes, one with high-resolution ($\sim 1''$) and ~ 1000 cm^2 collecting area, to be used for imaging and high resolution spectroscopy and the other of moderate resolution ($\sim 5''$) and 5000 cm^2 collecting area to be used for polarimetry, low resolution spectroscopy and for low noise-high sensitivity applications. A schematic of a possible payload is shown in Figure 21. The experiment could be launched from a Titan-3c and it might be possible to station-keep the experiment from a nearby manned orbiting workshop. Station-keeping allows the use of film and cryogenics, and the possibility of replacing the focal plane instruments.

11. Summary

Based on present knowledge, the instruments available for observations in X-ray astronomy are capable of several orders of magnitude improvement compared to what is actually being attained at the present time. These improvements include detection of very faint sources, high resolution imaging, spectroscopy and polarimetry. The only real limitation to the application of these instruments is the availability of space-borne platforms. It is also noteworthy that the principal requirements on these space platforms is weight-carrying capability. The stability, maneuvring, and data transmission requirements are typically less stringent than what now seems to be routinely accomplished in many satellite programs. Furthermore, one does not require exotic orbits; the most desirable place for an X-ray astronomy experiment is near the equator and at low altitude where we obtain the maximum shielding from cosmic rays by the terrestrial magnetic field and is still out of the regions of trapped radiation.

Acknowledgements

I wish to acknowledge the assistance that I have had with the astronomy group at

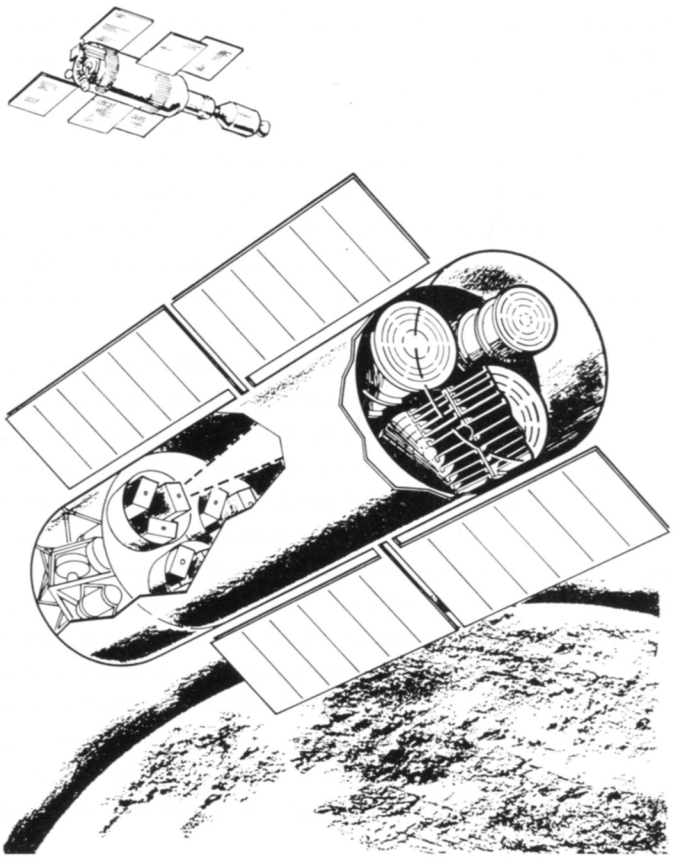

Fig. 21. Conceptual drawing of a large X-ray telescope facility where telescope is shared by several users.

AS&E with preparation of the report and in particular with Drs. Gorenstein and Kellogg for their contributions in the area of conventional X-ray astronomy experiments, and Drs. Vaiana, Van Speybroeck and Zehnpfennig for their contributions in the area of telescope techniques. I have also benefited from discussions with Dr. Giacconi and Professor Rossi of MIT regarding the contents of the paper.

Also, I wish to thank Professor Peterson, University of California, San Diego, Dr. Seward, Lawrence Radiation Laboratory, and Professor Bunner, University of Wisconsin, for providing material that I have used in this paper.

References

[1] Giacconi, R., Gursky, H., and Van Speybroeck, L.: 1968, *Ann. Rev. Astron. Astrophys.* **6**, 373.
[2] Giacconi, R., Reidy, W., Vaiana, G., Van Speybroeck, L., and Zehnpfennig, T.: 1969, *Space Sci. Rev.* **9**, 3.
[3] Bell, K. L. and Kingston, A. E.: 1967, *Monthly Notices Roy. Astron. Soc.* **136**, 241.
[4] Bowyer, C. S., Field, G. B., and Mack, J. E.: 1968, *Nature* **217**, 32.

[5] Mathieson, E. and Sanford, P. W.: 1964, in *Proceedings of the International Symposium on Nuclear Electronics, Paris, 1963,* ENEA, p. 65.
[6] Gorenstein, P. and Mickiewicz, S.: 1968, *Rev. Sci. Inst.* **39**, 816.
[7] Henry, R. C., Fritz, G., Meekins, J. F., Friedman, H., and Byram, E. T.: 1968, *Astrophys. J.* **153**, L11.
[8] Baxter, A. J., Wilson, B. G., and Green, D. W.: 1969, *Astrophys. J.* **155**, L145.
[9] Oda, M.: 1965, *Appl. Opt.* **4**, 143.
[10] Gursky, H., Giacconi, R., Gorenstein, P., Waters, J. R., Oda, M., Bradt, H., Garmire, G., and Sreekantan, B. V.: 1966, *Astrophys. J.* **146**, 311.
[11] Bradt, H., Garmire, G., Oda, M., Spada, G., Sreekantan, B. V., Gorenstein, P., and Gursky, H.: 1968, *Space Sci. Rev.* **8**, 471.
[11a] Gorenstein, P., Gursky, H., and Garmire, G.: 1968, *Astrophys. J.* **153**, 885.
[12] Schnopper, H. W., Thompson, R. I., and Watt, S.: 1968, *Space Sci. Rev.* **8**, 534.
[13] Ables, J. G.: 1969, *Astrophys. J.* **155**, L27.
[14] Tucker, W. H.: 1967, *Astrophys. J.* **148**, 745.
[15] Fritz, G., Meekins, J. F., Henry, R. C., Bryam, E. T., and Friedman, H.: 1968, *Astrophys. J.* **153**, L199.
[16] Angel, J. R. R., Novick, R., Vanden Bout, P., and Wolf, R.: 1969, *Phys. Rev. Letters* **22**, 861.
[17] Wolter, H.: 1952, *Ann. Phys.* **10**, 94.
[18] Giacconi, R. and Rossi, B.: 1960, *J. Geophys. Res.* **65**, 773.
[19] Vaiana, G., Rossi, B., Zehnpfennig, T., Van Speybroeck, L., and Giacconi, R.: 1968, *Science* **161**, 564.
[20] Underwood, J. H. and Muney, W. S.: 1967, *Solar Phys.* **1**, 129.
[21] Schnopper, H. and Kalata, K.: 1969, *Appl. Phys. Letters* **15**, 134.
[22] Gursky, H. and Zehnpfennig, T.: 1966, *Appl. Opt.* **5**, 875.